

## Hopping conduction in a "superlattice"\*

R. Tsu and G. Döhler†

IBM Thomas J. Watson Research Center, Yorktown Heights, New York 10598

(Received 13 November 1974)

We have used the formulation for the "Stark ladder," and a two-well model to describe hopping conduction via acoustical phonons in a "superlattice." Results show that negative differential conductance may occur when the "Stark-ladder" energy  $eFd$  is greater than the energy bandwidth. The mechanism is due to the fact that the transition probability at high fields decreases with the increase of  $F$ , because the electronic wave functions become more localized.

### I. INTRODUCTION

The transport properties in a man-made superlattice exhibiting negative differential conductance, have been theoretically<sup>1,2</sup> and experimentally studied.<sup>3</sup> The presence of an additional periodic potential produced by varying the alloy composition of two semiconductors, such as GaAs and GaAlAs, along one direction with a period of approximately 100 Å, results in a splitting of the conduction and valence bands into several minibands. If the mean free path is longer than the period of the superlattice, Bragg scattering from the minizone boundaries may give rise to "Bloch oscillation" and negative differential conductance. On the other hand, if the applied voltage is strong enough, Zener tunneling between minibands also leads to a current peak. It has been shown<sup>4,5</sup> that the energy states under extremely large electric fields form equally spaced discrete levels, the so-called "Stark ladder," if the interband matrix elements may be kept negligibly small. The corresponding wave functions are localized. Electrons may be transported via hopping or tunneling. Let us dwell on this point to further clarify the nature of conduction at high electric fields.

If the mean free path is not sufficiently long, the required field for the carriers to reach Bloch oscillation is so high that the Stark-ladder energy  $eFd$  is greater than the energy bandwidth of the minizone and the quasiclassical theory<sup>1</sup> becomes nonviable. The wave function under high fields are extremely localized; however negative differential conduction is still possible due to hopping conduction when  $eFd$  is less than the separation between the first and next minibands. Electrons from a given cell may hop via phonon emission and absorption to adjacent cells.<sup>6</sup> Because of the decrease in the overlap of the wave functions as  $F$  is increased, probability of hopping decreases. Resonant tunneling may take place whenever  $eFd$  coincides with the separation between the lowest and next minibands. Without intracellular relaxa-

tion, unlike the case of few barriers treated by Tsu and Esaki,<sup>7</sup> this process merely transfers the electrons from the ground level to the next level. Thus transport in this case is mainly determined by the intracellular relaxation. In this paper, our main purpose is to calculate the transport properties when  $eFd$  may be greater than the energy bandwidth of the first miniband but less than the separation between minibands. The latter case is more difficult to treat because of the resonant nature and a perturbation calculation is usually not valid.

Figure 1 shows possible transitions between electrons localized in a given cell to an adjacent cell. Under the application of a constant electric field, a constant potential energy difference exists between adjacent cells and a ladder structure for the energy states appears. If  $eFd$  in Fig. 1 is such that the level 1 coincides with level 2', electrons may tunnel resonantly from 1 to 2' marked by (a), followed by an inelastic scattering process marked by (b) to level 1', in order to repeat the process onto the next cell. This process has been treated by Kazarinov and Suris.<sup>2</sup> Observation of negative differential conductance in a GaAs-GaAlAs superlattice by Esaki and Chang is explained by this type of resonant-tunneling process.<sup>7</sup>

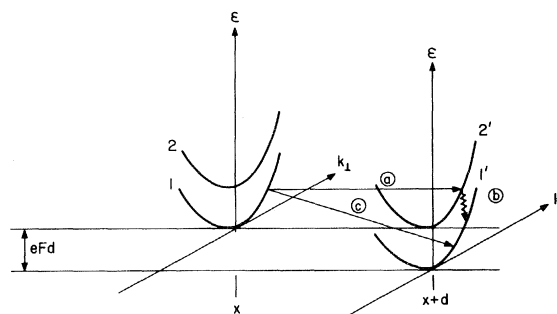


FIG. 1. Energy states under an applied field  $F$ . Process (a) involves direct tunneling followed by an inelastic scattering (b), and process (c) involves inelastic scattering.

In this paper, we treat the direct inelastic process from 1 to 1' denoted by (c) in Fig. 1, neglecting the presence of other states such as 2 and 2', etc. Our results show that negative differential conductance can take place. In Sec. II, hopping conduction is calculated from the use of the so-called "Kane functions"<sup>8</sup> applicable for a periodic system under a high electric field. If the electron mean free path is not much greater than the period  $d$ , the transfer of electrons from one cell to the next may be approximated by a "two-well model," which is treated in Sec. III. At high fields, the superlattice and two-well models give almost identical results. This is not too surprising since the wave function for the superlattice is extremely localized at high electric fields.

## II. HOPPING CONDUCTION IN A SUPERLATTICE VIA PHONONS

We shall use the solution of the Schrödinger equation in the presence of a static electric field  $F$ , when interband terms are negligible. Perturbation calculation is used for electron-phonon interaction. Our results are not applicable for the case of resonant tunneling because perturbation calculation is not valid generally for resonant case. Following Callaway,<sup>9</sup> the wave function  $\psi(\vec{r})$  may be written in the crystal-momentum representations

$$\psi(\vec{r}) = \sum_n \int \phi_n(\vec{k}) \psi_n(\vec{k}) d\vec{k}, \quad (1)$$

where

$$\psi_n(\vec{k}) = U_n(\vec{k}, \vec{r}) e^{i\vec{k} \cdot \vec{r}} \quad (2)$$

$$\psi(\vec{r}) = \left(\frac{d}{2\pi}\right)^{1/2} e^{i\vec{k} \cdot \vec{r}} \int_{-\pi/d}^{\pi/d} U(k_x, x) \exp \left\{ i \left[ k_x(x - \nu d - L) - \left(\frac{\epsilon_1}{2eFd}\right) \sin k_x d \right] \right\} dk_x. \quad (9)$$

For large  $F$ , this wave function is highly localized with  $\Delta x \sim \epsilon_1/eF$ , and centered at  $x = L + \nu d$ . In order for this formulation to be meaningful, the electron mean free path should be greater than  $\Delta x$ .

The current due to an electron in the cell  $\nu$  (energy state  $\nu$ ) making a hop to the cell  $\nu'$  (energy state  $\nu'$ ) is

$$j_{\nu\nu'} = \sum_{\vec{k}, \vec{k}'} e(\nu' - \nu) d [f(1 - f') \omega_{\nu\nu'} - f'(1 - f) \omega_{\nu'\nu}], \quad (10)$$

where  $f \equiv f(\epsilon_\nu - \mu_\nu)$  and  $f' \equiv f(\epsilon_{\nu'} - \mu_{\nu'})$ , in which

$$\phi_n(\vec{k}) = \left(\frac{d}{2\pi}\right)^{1/2} \exp \left( -\frac{i}{eF} \int_0^{k_x} [\epsilon - \epsilon_n^{(1)}(\vec{k}')] dk'_x \right) \times \delta(k_y - k'_y) \delta(k_z - k'_z), \quad (3)$$

$$\epsilon_n^{(1)}(\vec{k}) = eFX_{nn} + \epsilon_n(\vec{k}), \quad (4)$$

in which

$$X_{nn} \equiv \frac{(2\pi)^3}{V_0} i \int U_n^* \frac{\partial U_n}{\partial k_x} d\vec{r},$$

and  $\epsilon_n(\vec{k})$  is the energy of the  $n$ th band. The requirement that  $\phi_n(\vec{k})$  is periodic in  $\vec{k}$ , gives rise to the quantized levels

$$\epsilon_{\nu,n}(\vec{k}) = \nu eFd + \frac{d}{2\pi} \int_{-\pi/d}^{\pi/d} [\epsilon_n(\vec{k}) + eFX_{nn}] dk_x, \quad (5)$$

with  $\nu$  being any integer. Because of the periodic nature of  $U_n$ , the second term in the integral is a real constant term. We shall consider a one-band tight-binding model where

$$\epsilon_n(\vec{k}) \equiv \epsilon(\vec{k}) = \hbar^2 k_\perp^2 / 2m + \epsilon_0 - (\frac{1}{2} \epsilon_1) \cos k_x d, \quad (6)$$

then

$$\epsilon_{\nu}(\vec{k}) = \hbar^2 k_\perp^2 / 2m + \epsilon_0 + eFd(\nu + L/d), \quad (7)$$

where  $L$  is a constant coming from the  $X_{nn}$  term. The function  $\phi_\nu$  is then

$$\phi_\nu = \left(\frac{d}{2\pi}\right)^{1/2} \times \exp \left\{ -i \left[ k_x(\nu d + L) + \left(\frac{\epsilon_1}{2eFd}\right) \sin k_x d \right] \right\}. \quad (8)$$

Furthermore, we shall neglect the periodicity of the real lattice, but not that of the superlattice, i.e.,

$$U(\vec{k}, \vec{r}) = U(k_x, x),$$

where  $k_x$  is restricted within the minizone from  $-\pi/d$  to  $\pi/d$ , then

$\mu_\nu$  and  $\mu_{\nu'}$  are the chemical potentials, and  $\omega_{\nu\nu'}$  is the transition probability. In our calculation, equilibrium Fermi distribution has been used for  $f$  and  $f'$ . This is a fair approximation if the intracellular relaxation is much faster than intercellular hopping. Since

$$\omega_{\nu\nu'} = \omega_{\nu'\nu} e^{\beta(\epsilon_\nu - \epsilon_{\nu'})},$$

Eq. (10) becomes

$$j_{\nu\nu'} = \sum_{\vec{k}, \vec{k}'} e(\nu' - \nu) df(1 - f') \omega_{\nu\nu'}^\mp (1 - e^{-\beta(\nu' - \nu)eFd}), \quad (11)$$

with  $\beta \equiv (k_B T)^{-1}$ . The  $(-)$  sign is for phonon emission and  $(+)$  sign is for phonon absorption. The total current is the sum of both emission and absorption processes, although for convenience, we have not explicitly indicated the sum in Eq. (11). Using the "golden rule," the transition probability

$$\omega_{\nu\nu'}^{\mp}(\vec{k}_\perp, \vec{k}'_\perp) = \frac{2\pi}{\hbar} \sum_{\vec{q}} |\langle \nu', \vec{k}'_\perp, n_{\vec{q}} \pm 1 | H_{ep} | \nu, \vec{k}_\perp, n_{\vec{q}} \rangle|^2 \times \delta(\epsilon_\nu(\vec{k}_\perp) - \epsilon_{\nu'}(\vec{k}'_\perp) \mp \hbar\omega_{\vec{q}}). \quad (12)$$

The matrix element for electron-phonon interaction may be written

$$\langle \nu', \vec{k}'_\perp, n_{\vec{q}} \mp 1 | H_{ep} | \nu, \vec{k}_\perp, n_{\vec{q}} \rangle = C(q) \langle \nu', \vec{k}'_\perp | e^{i\vec{q}\cdot\vec{r}} | \nu, \vec{k}_\perp \rangle (n_{\vec{q}} + \frac{1}{2} \pm \frac{1}{2})^{1/2}, \quad (13)$$

where  $C(q)$ ,<sup>10</sup> for the acoustical phonon, is  $iC_1(|q|/2\rho C_s)^{1/2}$ , with  $\rho$ ,  $C_1$ , and  $C_s$  being the density, the deformation potential, and the longitudinal velocity of sound, respectively. The matrix element

$$\begin{aligned} \langle | e^{i\vec{q}\cdot\vec{r}} \rangle &= \int_{-\pi/a}^{\pi/a - \hat{q}_x} \phi_{\nu'}^*(\vec{k} + \vec{q}) \phi_\nu(\vec{k}) U_m dk_x \\ &+ \int_{\pi/a - \hat{q}_x}^{\pi/a} \phi_{\nu'}^*(\vec{k} + \vec{q}) \phi_\nu(\vec{k}) U_{m+1} dk_x \\ &\equiv I_1(\hat{q}_x) U_m + I_2(\hat{q}_x) U_{m+1}, \end{aligned} \quad (14)$$

where  $U_m$  and  $U_{m+1}$  are defined in Appendix A, and  $\hat{q}_x \equiv q_x - 2\pi m/d$ , which states that  $\hat{q}_x$  is also restricted to the first minizone. Using the wave function of Eq. (9), we find that

$$I_1 = \begin{cases} J_{\nu'-\nu} \left( \frac{\epsilon_1}{eFd} \sin \frac{\hat{q}_x d}{2} \right) & \text{for } \hat{q}_x = 0, \\ 0 & \text{for } \hat{q}_x = 2\pi/d \end{cases}$$

and

$$I_2 = \begin{cases} 0 & \text{for } \hat{q}_x = 0 \\ J_{\nu'-\nu} \left( \frac{\epsilon_1}{eFd} \sin \frac{\hat{q}_x d}{2} \right) & \text{for } \hat{q}_x = 2\pi/d \end{cases}$$

---


$$\begin{aligned} \langle | e^{i\vec{q}_x \cdot \vec{r}} \rangle_{\gamma, m} &= J_\gamma \left( \frac{\epsilon_1}{eFd} \sin \frac{\hat{q}_x d}{2} \right) \left( U_m + \frac{\hat{q}_x d}{2} (U_{m+1} - U_m) \right) \sim J_\gamma \left( \frac{\epsilon_1}{eFd} \sin \frac{q_x d}{2} \right) \frac{\sin \frac{1}{2} q_x W}{\frac{1}{2} q_x W} \frac{1}{1 - (q_x W / 2\pi)^2} \\ &\equiv \langle | \rangle_{\gamma q_x}, \end{aligned} \quad (17)$$

so that

$$\omega_{\gamma, \vec{k}_\perp}^{\mp} = \frac{1}{(2\pi)^3} \int_{-q_x \max}^{q_x \max} dq_x \int_0^{2\pi} d\theta \frac{2\pi}{\hbar} \frac{C_1^2 |q|}{2C_{s\rho}} \times (n_{\vec{q}} + \frac{1}{2} \pm \frac{1}{2}) 2\pi |\langle | \rangle_{\gamma, q_x}|^2, \quad (18)$$

where for  $\omega_\gamma^{\pm}$ ,  $q_{x \max} = \pi/a$

where  $J_{\nu'-\nu}$  is the Bessel function of the order  $\nu' - \nu$ . In order to facilitate computation, we approximate

$$I_1 \sim (1 - \hat{q}_x d / 2\pi) J_{\nu'-\nu}$$

and

$$I_2 \sim (\hat{q}_x d / 2\pi) J_{\nu'-\nu}.$$

Then the approximate matrix element becomes

$$\begin{aligned} \langle | e^{i\vec{q}\cdot\vec{r}} \rangle &\sim \delta_{\vec{k}'_\perp, \vec{k}_\perp + \vec{q}_\perp} J_\gamma \left( \frac{\epsilon_1}{eFd} \sin \frac{\hat{q}_x d}{2} \right) \\ &\times \left( U_m + \frac{\hat{q}_x d}{2\pi} (U_{m+1} - U_m) \right), \end{aligned} \quad (15)$$

where  $\gamma = \nu' - \nu$ . To find the total transition probability from Eq. (12) for  $\omega_{\nu\nu'}$ , we need to sum over  $\vec{q}$  within the minizone, and  $m$  from 0 to  $d/a$ , with  $a$  being the lattice constant of the semiconductor. Because of the energy  $\delta$  function in Eq. (12), and the transverse momentum  $\delta$  function in Eq. (15), we have the conditions

$$eFd(\nu - \nu') + \frac{\hbar^2}{2m} (k_\perp^2 - k_\perp'^2) \mp \hbar\omega_{\vec{q}} = 0, \quad (16a)$$

and

$$q_\perp^2 = k_\perp'^2 + k_\perp^2 - 2k'_\perp k_\perp \cos \theta. \quad (16b)$$

Given the specific dispersion relation for the phonons, we may solve for  $q$  as a function of  $V$ ,  $k_\perp$ ,  $\hat{q}_x$ , and  $\theta$ , with  $V \equiv eFd(\nu - \nu')$ . In principle, we may now compute  $\omega_{\nu\nu'}(k_\perp)$  by integrations on  $\theta$  and  $\hat{q}_x$  together with summation on  $m$ . The total current is now obtained by summing over  $\vec{k}_\perp$  for both phonon-emission and phonon-absorption processes, and  $\nu' - \nu = 1, 2, 3, \dots$ . Since the computation is still a rather formidable task, a number of approximations have been used to simplify our computations. First, we assume that the dispersion of acoustical phonons is represented by a constant speed of sound. Instead of summing on  $\hat{q}_x$  in the minizone and sum over all the minizone, we replace the process by an integration on  $q_x$  in the extended reciprocal space. It may be shown that

and for  $\omega_\gamma^+$

$$q_{x \max} = \begin{cases} (eFd\gamma + \hbar^2 k_\perp^2 / 2m) / \hbar C_s & \text{if } eF\gamma + \hbar^2 k_\perp^2 / 2m < \omega_{ac} \\ \pi/a & \text{if } eF\gamma + \hbar^2 k_\perp^2 / 2m \geq \omega_{ac} \end{cases}$$

in which  $\omega_{ac}$  is the cutoff frequency for acoustical phonons. As pointed out earlier, due to the small intercellular transition in comparison to the intracellular relaxation, prior to and after a transition is made, both the phonon and electron populations are governed by the equilibrium distribution functions, i.e., Bose-Einstein and Fermi-Dirac functions, respectively. The computation may be greatly simplified if we assume  $f' \sim 0$  in Eq. (11), because  $\epsilon_{\nu'} - \mu_{\nu'} \gg k_B T$ . Replacing the sum on  $\vec{k}$  to an integration on energy with the density of states

$$N(\epsilon_{\nu}) = (m/\pi\hbar^2) \Theta(\epsilon_{\nu} - \epsilon_{\nu}(k_{\perp} = 0)),$$

we have

$$j_{\gamma} = \frac{em\gamma}{\pi\hbar^2} \int_0^{\infty} [\omega_{\gamma}^+(\epsilon_{\perp}) + \omega_{\gamma}^-(\epsilon_{\perp})] \times f(\epsilon_{\perp})(1 - e^{-\beta\gamma eFd}) d\epsilon_{\perp}. \quad (19)$$

### III. TWO-WELL MODEL

If the barrier is such that the tunneling probability from one well to the next-nearest cell may be neglected, we may consider only the net phonon-assisted transitions between the neighboring cells. Our purpose is to derive the hopping current for this limiting case and compare the results with those of Sec. II. A general treatment for large tunneling between cells and long mean free path, is given in Appendix B.

Figure 2 shows a section of the superlattice potential profile. We assume that all the energy states other than the lowest levels denoted by  $\lambda_1$  and  $\lambda_2$  are far away, so that it is meaningful to consider the lowest states only. When the barrier width  $l$  is large, electron wave functions do not overlap, so that

$$H_0|1\rangle = \lambda_1|1\rangle, \quad H_0|2\rangle = \lambda_2|2\rangle,$$

and  $\lambda_1 - \lambda_2 = V$ . Obviously for very high field, the next level  $\Lambda_2$  may be brought to the vicinity of

$\lambda_1$ , so that level  $\lambda_1$  will be coupled to  $\Lambda_2$  more so than with  $\lambda_2$ . This belongs to the resonant tunneling case. As  $l$  is reduced, electrons in the states  $\lambda_1$  and  $\lambda_2$  are coupled so that

$$\epsilon_{1,2} = \lambda_0 \pm \left[ \left( \frac{V}{2} \right)^2 + \alpha^2 \right]^{1/2} + \frac{\hbar^2 k_{\perp}^2}{2m}, \quad (20)$$

where  $\alpha \equiv \langle 1|H_1|2\rangle$ , and  $\lambda_0$  is the longitudinal energy when  $V=0$ , and  $\alpha=0$ , in which  $H_1$  is the coupling operator. Note that  $2\alpha$  is the splitting for  $V=0$ . These two states have wave functions

$$\begin{aligned} \epsilon_1: \quad \psi_1 &= \left( \frac{1}{1+b^2} \right)^{1/2} (|1\rangle + b|2\rangle), \\ \epsilon_2: \quad \psi_2 &= \left( \frac{1}{1+b^2} \right)^{1/2} (b|1\rangle - |2\rangle), \end{aligned} \quad (21)$$

where

$$b \equiv \left[ 1 + \left( \frac{V}{2\alpha} \right)^2 \right]^{1/2} - \frac{V}{2\alpha}. \quad (22)$$

If we let

$$|1\rangle \propto \sin(p\pi/W)(x + \frac{1}{2}l)e^{ik_{\perp}p} \quad (23)$$

and

$$|2\rangle \propto \sin(p\pi/W)(x - \frac{1}{2}l)e^{ik_{\perp}p},$$

the matrix element

$$\begin{aligned} \langle \psi_1 | e^{i\vec{q}\cdot\vec{r}} | \psi_2 \rangle &= \frac{i2b}{1+b^2} \frac{1}{q_x W} \sin \frac{q_x d}{2} \sin \frac{q_x W}{2} \\ &\times \frac{1}{1 - (q_x W/2\pi)^2} \delta_{\vec{k}_1, \vec{k}_1 + \vec{q}_1}. \end{aligned} \quad (24)$$

For  $p=1$  (ground state), and  $V \gg 2\alpha$ ,

$$\begin{aligned} \langle \psi_1 | e^{iq_x x} | \psi_2 \rangle &= \frac{i2\alpha}{V} \sin \left( \frac{q_x d}{2} \right) \frac{1}{q_x W} \\ &\times \frac{\sin(\frac{1}{2}q_x w)}{1 - (q_x W/2\pi)^2}, \end{aligned} \quad (25)$$

which is identical to Eq. (17) when  $eFd \gg \epsilon_1$ , if

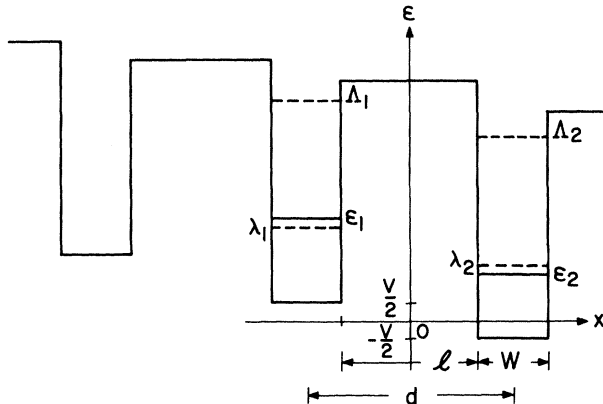


FIG. 2. Section of the superlattice potential profile,  $\lambda_1$ ,  $\lambda_2$ ,  $\Lambda_1$ , and  $\Lambda_2$  are the energies of the uncoupled wells with width  $W$ .  $\epsilon_1$  and  $\epsilon_2$  are the energies of the coupled wells when the coupling is increased by decreasing the barrier width  $l$ .

we identify  $\epsilon_1 = 2\alpha$ ,  $eFd = V$ , and  $J_1(\delta) \sim \frac{1}{2} \delta$ . The transition probability via electron-phonon interaction is then

$$w_{12}^{\mp} = \frac{2\pi}{\hbar} \sum_{\mathbf{q}} |\langle \psi_1 | | \psi_2 \rangle|^2 \delta(\epsilon_1(\mathbf{k}_{\perp}) - \epsilon_2(\mathbf{k}'_{\perp}) \mp \hbar \omega_{\mathbf{q}}^{\pm}). \quad (26)$$

The rest of the calculation is identical to Sec. II. The validity of the two-well model depends on the extent of the localization of the wave functions, therefore it is generally not applicable for low electric fields. Although the two-well model is only correct at high fields, the approach may be used to treat the resonant tunneling case more easily, because at least in principle, as many higher levels as one wants may be incorporated into the formulation.

#### IV. RESULTS AND DISCUSSIONS

We have computed a number of cases using  $\epsilon_1$  and temperature as parameters for the well width  $W = \frac{1}{2}d$ , and  $d = 50 \text{ \AA}$ . Figure 3 shows the transition probability for phonon emission at  $300^\circ\text{K}$  as a function of  $F$ , at a given fixed transverse energy  $\epsilon_{\perp} = \hbar^2 k_{\perp}^2 / 2m = 0.1 \text{ eV}$ . The asymptote for large  $F$  is proportional to  $F^{-2}$ . For the two-well model, the asymptotes meet the horizontal asymptotes near  $V = 0.01, 0.02$ , and  $0.1 \text{ eV}$ , respectively for the cases of  $\epsilon_1 = 0.01, 0.02$ , and  $0.1 \text{ eV}$ . The curves for  $\omega_{\gamma=1}(\epsilon_{\perp} = 0.1 \text{ eV})$  are denoted by superlattice (1). In other words for  $\gamma = 1$ , we only consider the case for transitions between the adjacent cells. Note that these curves are oscillatory at low fields and have

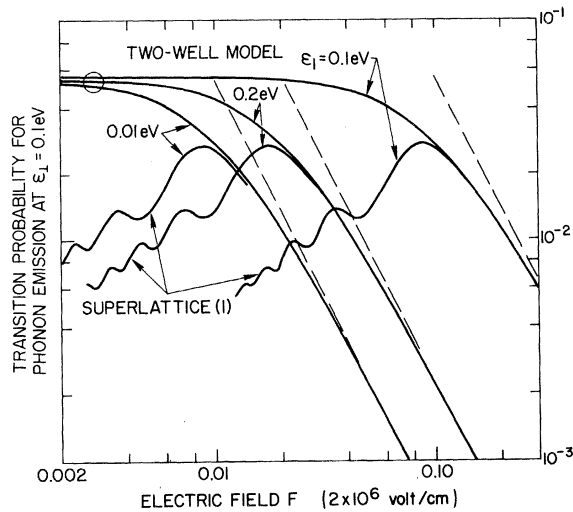


FIG. 3. Transition probability for phonon emission at  $\epsilon_{\perp} = 0.1 \text{ eV}$ ,  $\omega^{\pm} \times 4\pi C_s \rho \hbar / C_1^2 \text{ v F}$  vs the applied electric field  $F$  at  $300^\circ\text{K}$ .

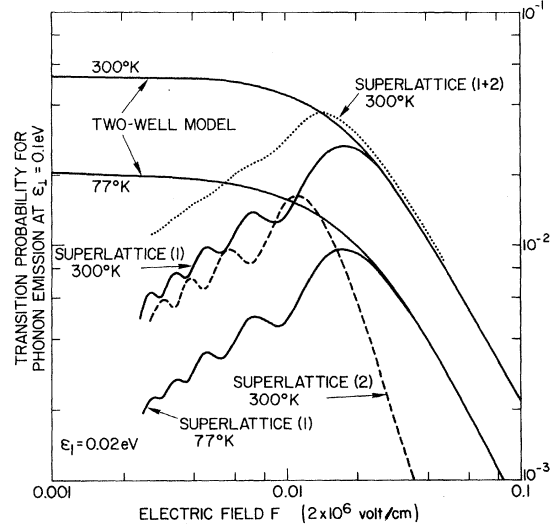


FIG. 4. Comparisons between the superlattice case and the two-well model for  $\omega^{\pm} \times 4\pi C_s \rho \hbar / C_1^2 \text{ v F}$  at  $300$  and  $77^\circ\text{K}$ .

peaks near  $eFd \sim \epsilon_1$  and asymptotically approach those for the two-well model. The low-field oscillatory behavior, having extrema whenever the energy bandwidth becomes integral multiples of the Stark ladder energy, may be eliminated when the transitions involving next-nearest neighbors are taken into account. The dashed curve in Fig. 4 is for  $\omega_{\gamma=2}(\epsilon_{\perp} = 0.1 \text{ eV})$ , and the sum  $\omega_{\gamma=1}^{\pm} + \omega_{\gamma=2}^{\pm}$  is denoted by superlattice (1+2), shown as a dotted curve where the oscillation has been almost eliminated. Decreasing temperature to  $77^\circ\text{K}$  does not produce a significant shift of the peak position. Figure 5 shows the hopping current as a function of the applied field. As pointed out in the caption, the Fermi level only enters as a prefactor. This is because we have further approximated the Fermi function for  $\epsilon_0 - \epsilon_{f_0} \gg k_b T$ . The curves denoted as superlattice (1), superlattice (2), and superlattice (1+2) are for  $j_{\gamma=1}$ ,  $j_{\gamma=2}$ , and  $j_1 + j_2$ . Again the oscillatory behavior at low fields is almost eliminated by taking into account the hopping involving next-nearest neighbors. The comparable case for the two-well model is shown as solid curve marked "two-well model." In order to examine more closely the effects of temperature and bandwidth  $\epsilon_1$  on the position for the peak current, we have computed few cases for the temperatures,  $300$  and  $77^\circ\text{K}$ , corresponding to a range of  $\epsilon_1$ , much smaller to much greater than  $k_b T$ . The results are shown in Fig. 6. There is no simple relationship as a whole, only a general tendency. For instance, for  $\epsilon_1 = 0.01 \text{ eV}$  at  $300^\circ\text{K}$ , maximum occurs around  $eFd = 0.009 \text{ eV}$  which indicated that the peak is close to the point  $\epsilon_1 \sim 0.01 \text{ eV}$ ; however, at  $77^\circ\text{K}$ ,

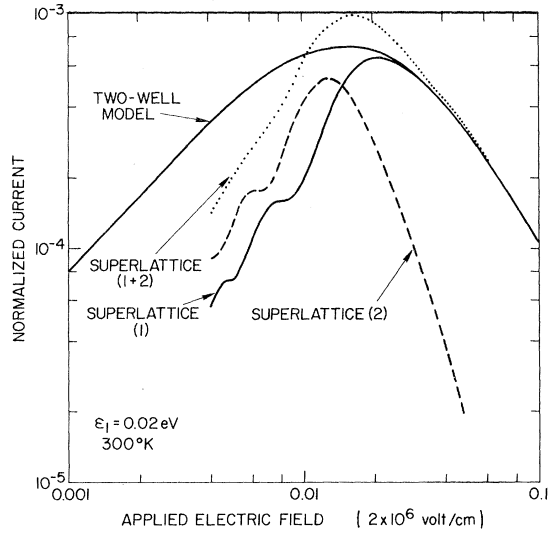


FIG. 5. Normalized current vs  $F$ . The dotted curve is the sum of the currents due to the hopping between the nearest neighbor marked as superlattice (1) and that of the next nearest neighbor masked as superlattice (2). A factor  $e(C_1/2\pi\hbar)^2(m/\hbar C_s\rho) \exp[(\epsilon_{F0}-\epsilon_0)/k_B T]$ , should be used to obtain the actual current, where  $\epsilon_0$  and  $\epsilon_{F0}$  are the longitudinal energy and the Fermi level, respectively.

the peak is moved down to  $eFd=0.0065$  eV. For very wide bandwidth,  $\epsilon_1=0.1$  eV, the peak for 300°K is located near  $eFd\sim 0.05$  eV, but at 77°K, it moves down to  $\sim 0.025$  eV. Thus, we conclude that the peak position is moved to lower fields either by reducing  $\epsilon_1$  or  $k_B T$ , although the temperature effect is generally smaller. At high fields, the asymptotic value of the current is proportional to  $F^{-s}$ , where  $s>1$ . Note that negative differential conductivity will not occur until  $F>10^5$  V/cm for relatively large  $\epsilon_1\sim 0.1$  eV, and high temperature, 300°K. Thus, negative differential conductivity may not occur at all if other mechanisms were considered.

In conclusion, this type of negative differential conductivity will appear under the condition of fairly narrow energy bandwidth. The physical mechanism is due to the fact that the transition probability at high field is inversely proportional to the square of the field. The decrease of transition probability at high fields is due to the decrease of overlap for the electronic wave func-

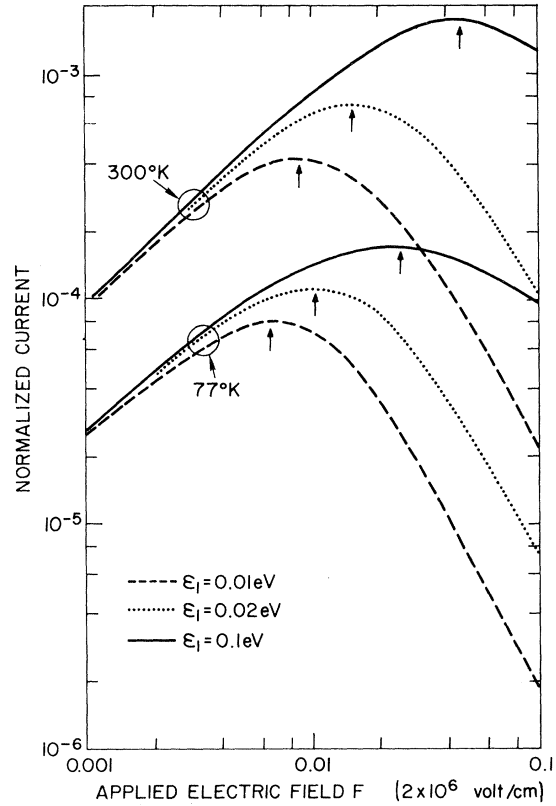


FIG. 6. Normalized current vs  $F$  for the two-well model at 300 and 77°K, for three values of the energy spitting at zero field,  $\epsilon_1=0.01, 0.02,$  and  $0.1$  eV.

tions. Suppose it is possible to observe negative differential conductivity for a real solid where  $a\sim 2$  Å and  $F\sim 5\times 10^6$  V/cm, we need an energy bandwidth  $\epsilon_1\sim eFa$ , in the neighborhood of 0.1 eV. It is highly unlikely that these requirements can be met by real solids. Some organic solids and layered compounds may meet our requirements if the mean free path were sufficiently long. For mean free path shorter than  $\Delta x\sim \epsilon_1/eF$ , our formulation in Sec. II breaks down. Due to the use of perturbation calculation, our results do not apply whenever the transition rates become comparable to the intracell relaxation rates.

ACKNOWLEDGMENT

It is a pleasure to acknowledge many helpful discussions with T. Schultz.

APPENDIX A

$$\int_{\text{vol}} e^{i(\vec{k}-\vec{k}'+\vec{q})\cdot\vec{r}} U^*(k_x', x) U(k_x, x) d\vec{r} = 2\pi\delta\left(k_x + q_x - k_x' - \frac{2\pi m}{d}\right) \delta_{\vec{k}'_{\perp}, \vec{k}_{\perp} + \vec{q}} U_m',$$

where

$$U_m \equiv \int_{\text{cell}} U^*(k_x', x) U(k_x, x) e^{i2\pi mx/d} dx.$$

Now  $k_x$  and  $k_x'$  are restricted to the first minizone, and  $2\pi m/d$  is the reciprocal-lattice vector. Taking

$$U(k_x, x) = U(x) = \begin{cases} (2/W)^{1/2} \cos(\pi x/w), & |x| \leq \frac{1}{2}W, \\ 0, & \frac{1}{2}W \leq |x| \leq \frac{1}{2}d, \\ U(x - pd), & pd - \frac{1}{2}d \leq |x| \leq pd + \frac{1}{2}d, \end{cases}$$

then

$$U_m = [\sin(m\pi W/d)/m\pi W/d][1 - (mW/d)^2]^{-1}.$$

#### APPENDIX B

If the tunneling probability between cells is large and the mean free path is long, for a system of  $N$  cells, we consider a more general case of  $P$  levels in a given cell  $\nu$ . When the separation between cells are large, we may assume that all the states  $|\nu, p\rangle$ , for a given state  $p$  in a given cell  $\nu$ , are known; i.e.,

$$H_0|\nu, p\rangle = \lambda_{\nu,p}|\nu, p\rangle,$$

where  $\nu = 1, \dots, N$ ; and  $p = 1, \dots, P$ . If the cells are now brought closer together so that  $\alpha_{\nu\nu', pp'}$  denotes couplings, the new energy states are given by the roots of the determinant

$$\det |(\lambda_{\nu,p} - \epsilon)\delta_{\nu\nu', pp'} + \sum_{\nu'', p''} \alpha_{\nu\nu'', pp''}(I - \delta_{\nu\nu'', pp''})| = 0,$$

and the eigenstates  $\psi_{\nu,p}$  can be obtained for each  $\epsilon_{\nu,p}$ . Because  $\lambda_{\nu,p} - \lambda_{\nu+1,p} = eFd$ , it is now possible to have resonant tunneling between adjacent cells, whenever  $\lambda_{\nu,p} - \lambda_{\nu,p'} = eFd$ .

\*Research sponsored in part under ARO contract.

†On leave from Max-Planck-Institute, Stuttgart.

<sup>1</sup>L. Esaki and R. Tsu, IBM J. Res. Develop. 14, 61 (1970); P. L. Lebowitz and R. Tsu, J. Appl. Phys. 41, 2664 (1970); P. J. Price, IBM J. Res. Develop. 17, 39 (1973).

<sup>2</sup>R. F. Kazarinov and R. A. Suris, Sov. Phys.-Semicond. 6, 120 (1972).

<sup>3</sup>L. Esaki, L. L. Chang, W. E. Howard, and V. L. Rideout, in *Proceedings of the Eleventh International Conference on the Physics of Semiconductors* (Polish Scientific, Warsaw, 1972), p. 431; L. Esaki and L. L. Chang, Phys. Rev. Lett. 33, 495 (1974).

<sup>4</sup>G. Wannier, *Elements of Solid State Theory* (Cambridge U. P., London, 1959), p. 66.

<sup>5</sup>H. Fukuyama, R. A. Bari, and H. C. Fogedby, Phys.

Rev. B 8, 5579 (1973).

<sup>6</sup>G. Döhler, R. Tsu, and L. Esaki, Solid State Commun. (to be published). This paper describes a mechanism for negative differential conductivity between states of the lowest miniband in adjacent wells via acoustical phonons, as well as via Coulomb scattering from impurities.

<sup>7</sup>R. Tsu and L. Esaki, Appl. Phys. Lett. 22, 562 (1973); L. L. Chang, L. Esaki, and R. Tsu, Appl. Phys. Lett. 24, 593 (1974).

<sup>8</sup>E. O. Kane, J. Phys. Chem. Solids 12, 181 (1959).

<sup>9</sup>J. Callaway, Phys. Rev. 130, 549 (1963).

<sup>10</sup>C. Kittel, *Quantum Theory of Solids* (Wiley, New York, London, 1963), Chap. 7.